Rheology and Photo-Cross-Linking of Thiol−Ene Polymers

Bor-Sen Chiou, Robert J. English, and Saad A. Khan*

Department of Chemical Engineering, North Carolina State University, Raleigh, North Carolina 27695-7905

Received March 14, 1996; Revised Manuscript Received May 30, 1996[⊗]

ABSTRACT: A dynamic rheological technique, Fourier transform mechanical spectroscopy (FTMS), was used to monitor in real time the evolving rheological properties during UV cross-linking of two thiol−ene systems. These systems comprised a trifunctional thiol (trimethylolpropane tris(2-mercaptoacetate)) together with a trifunctional allyl monomer (triallyl isocyanurate) and a tetrafunctional thiol (pentaerythritol tetrakis(2-mercaptoacetate)) with the same allyl monomer. FTMS, in conjunction with specially designed quartz plates, provided an *in situ* method to elucidate the effects of temperature and monomer functionality on the photoinitiated polymerization of these systems. It was found that the tetrafunctional thiol system cross-linked at a faster rate than the trifunctional thiol system over the temperature range (25−50 °C) studied. Moreover, increasing the temperature increased the cross-linking rates for both systems. The Winter−Chambon criterion was applied to determine the gel point and the two parameters which characterize the material at its gel point, the gel stiffness, S, and the relaxation exponent, n. The gel stiffness was found to be greater for the trifunctional thiol system, which was consistent with the higher value of conversion calculated from the Flory−Stockmayer theory of gelation. Relaxation exponents of 0.80 and 0.81−0.82 were determined for the tri- and tetrafunctional thiol systems, respectively, indicating similar fractal structures at the gel point. These relaxation exponents were also invariant over the temperature ranges studied, suggesting that the cross-linking mechanisms remained unchanged with temperature. From the temperature dependence of the gel times, apparent activation energies of 6.6 and 14 kcal/mol were calculated for the tri- and tetrafunctional thiol systems, respectively.

Introduction

Ultraviolet curing polymers have enjoyed widespread commercial growth over the past decade, due to the combined attributes of rapid, energy efficient curing and the possibility of achieving formulations free of volatile organic compounds (VOCs). Currently, acrylate-functional systems constitute the major share of UV-curable formulations, mainly due to their rapid curing via free radical polymerization. The range of commercially available prepolymers and monomeric diluents allows scope for variation of the material properties of the cured assembly across a wide latitude by tailoring both the acrylate functionality and the chemical architecture between the reactive groups. However, there has been a recent resurgence in interest in nonacrylate photopolymers, due to the increasingly stringent environmental and toxicological regulatory issues associated with acrylates.[1] This has led to renewed interest in thiol−ene compositions, which offer a toxicologically safer alternative to acrylate-functional systems.

The thiol−ene photoinitiated polymerization proceeds by a radical step-growth mechanism, in contrast to the chain propagation associated with acrylate-functional systems[2] (Figure 1). The photoinitiator (P) first absorbs UV radiation to produce an excited species (P*). This species then reacts with the thiol by hydrogen abstraction to produce the thiyl radical, R′−S•. Propagation then occurs in two steps: the radical addition of the thiyl radical to the olefin, producing an intermediate thioether carbon radical, R′−S−CH_2−$\dot{C}$H−R, which subsequently generates an additional thiyl radical via hydrogen abstraction, thus propagating the polymerization. If oxygen is present in the system, it is incorporated onto the network as a peroxy radical, which undergoes a chain-transfer reaction with thiol to give an oxygen addition product and regenerates the propagating species, the thiyl radical. Termination is believed to occur through the radical−radical recombination of the thioether carbon and/or thiyl radicals. Thus, polymerization of stoichiometric equivalents of a difunctional thiol and a difunctional −ene compound produces linear polymers. Increasing the functionality of either comonomer results in the formation of a three-dimensional, cross-linked network. One major advantage thiol−ene formulations offer over acrylate-functional systems is that they are not inhibited by oxygen.[1] Typical thiol-functional monomers include 3-mercaptopropionate esters or 2-mercaptoacetate esters of polyhydric alcohols. These materials are copolymerized in the presence of polyfunctional allyl ethers, allyl isocyanurates, or allyl-,

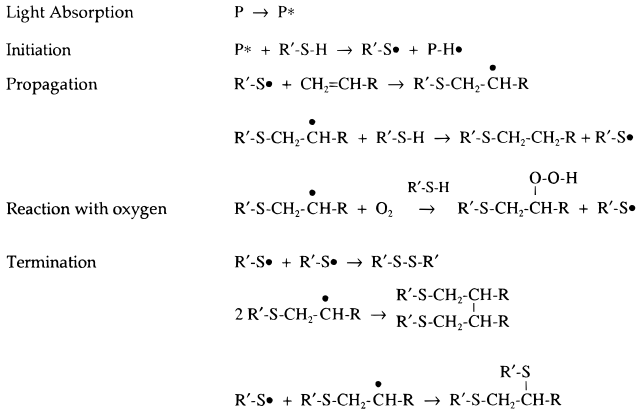

Figure 1. Schematic representation of the thiol−ene step-growth mechanism. The propagating species in this case is the thiyl radical, R′S•, which is initially generated from the corresponding thiol following hydrogen abstraction by a reactive species (P*) derived from the photoinitiator (P). Addition of the thiyl radical to the double bond of the unsaturated comonomer and subsequent hydrogen abstraction from a second thiol functionality generates a thioether linkage and regenerates the propagating species. There is no oxygen inhibition and termination is believed to occur through the radical−radical recombination of the thioether carbon and/or thiyl radicals.

* To whom correspondence should be addressed. Phone: 919-515-4519. Fax: 919-515-3465. E-mail: khan@che.ncsu.edu.

[⊗] Abstract published in *Advance ACS Abstracts,* July 1, 1996.

crotyl- or norbornenyl-terminated oligomers. Currently, thiol−ene formulations are utilized in a diverse range of applications, including adhesives for optical bonding, conformal coatings, and optical fiber coatings.[1]

Kinetic aspects of thiol−ene photoinitiated polymerizations have been studied by both differential scanning calorimetry[3,4] and Fourier transform infrared spectroscopy.[5] The final mechanical properties of the cured assembly have also been investigated.[5,6] However, there is a lack of studies in which the evolving rheological properties of the system are monitored during photoinitiated polymerization. The evolution of the rheological material properties directly reflects the kinetics of cross-linking, as dictated by both the extent and density of cross-links. Ultimately, the mode of assembly and topology of the network dictates the final properties of the cured assembly. The determination of how chemical architecture, such as monomer functionality, and processing parameter, such as temperature, influence the rheological properties during photoinitiated polymerization is also crucial for optimizing the curing process.

Fourier transform mechanical spectroscopy (FTMS) provides a method for monitoring the evolving rheological properties because it allows simultaneous measurement of the dynamic moduli at several frequencies during the course of photoinitiated polymerization. Dynamic rheological measurements, which are sensitive to the degree of cross-linking, have been used to accurately determine the gel point.[7] Winter and Chambon[8] have shown that at the gel point, both the elastic modulus (G') and the viscous modulus (G'') exhibit the same power-law variation with respect to the frequency of oscillation. The corresponding expressions describing the dynamic moduli at the gel point are as follows:

$$G'(\omega) = S\,\Gamma(1-n)\cos(n\pi/2)\,\omega^n \quad (1)$$

$$G''(\omega) = S\,\Gamma(1-n)\cos(n\pi/2)\tan(n\pi/2)\,\omega^n \quad (2)$$

$$0 < n < 1 \quad (3)$$

$$0 < \omega < 1/\lambda_0 \quad (4)$$

where n is the relaxation exponent, S is the gel stiffness, Γ is the gamma function, and ω is the frequency of oscillation. The frequency range for the power-law behavior is bounded by zero at the lower end and $1/\lambda_0$ at the high-frequency limit, where λ_0 is a characteristic time of the prepolymers which marks the transition to glassy behavior.[9] It follows from eqs 1 and 2 that the loss tangent, tan δ, becomes independent of frequency at the gel point:

$$\tan\delta = \frac{G''}{G'} = \tan\left(\frac{n\pi}{2}\right) \quad (5)$$

Therefore, the values of tan δ determined at different frequencies of oscillation, when plotted as a function of time, should converge at the gel time, t_{gel}.

In the present study, we use a novel, *in situ* technique[10] to monitor the evolving dynamic rheological properties during the photoinitiated polymerization of two model thiol−ene systems. These systems are composed of (i) a trifunctional thiol (trimethylolpropane tris(2-mercaptoacetate)) and a trifunctional allyl monomer (triallyl isocyanurate) and (ii) a tetrafunctional thiol (pentaerythritol tetrakis(2-mercaptoacetate)) with the same trifunctional allyl monomer (Figure 2). The effects of variation of both the thiol monomer functionality and the temperature on the photoinitiated polymerization kinetics of these systems are examined in this study. The gel times are also determined using the Winter−Chambon criterion, and the differences in the material properties at the gel point of the two systems are compared.

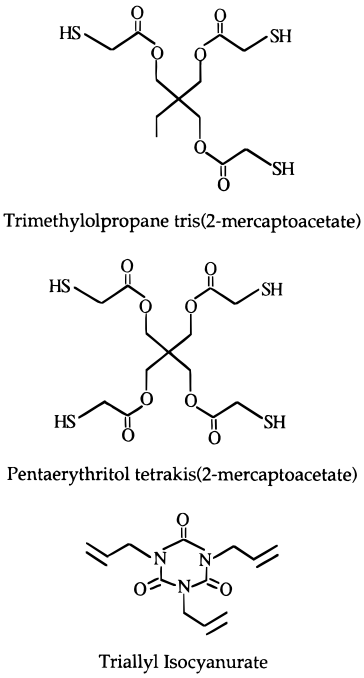

Figure 2. Schematic representation of the monomer utilized in the formulation of the thiol−ene systems. One system contains the trifunctional thiol and trifunctional allyl monomers, while the other system contains the tetrafunctional thiol and the same trifunctional allyl monomers.

Experimental Section

Sample Preparation. The model thiol−ene systems consisted of stoichiometrically equivalent combinations of both the trifunctional thiol and the tetrafunctional thiol with triallyl isocyanurate. The thiols were protected from oxidative polymerization by the addition of hydroquinone. The monomers and hydroquinone were purchased from Aldrich Chemicals and were used as received. Formulations were prepared by mixing the monomers for 5 min. A commercial photoinitiator, Esacure TZT (Sartomer Inc.), which comprised a blend of methylbenzophenones, was added at a level of 1.0% by weight of the monomers. Stirring was maintained for a further 5 min following the addition of the photoinitiator. The final formulations contained 0.31% by weight of hydroquinone. Samples were prepared immediately prior to each experiment, in order to ensure reproducibility of sample history. The glass transition temperatures of the samples following prolonged exposure (0.6 mW cm^{-2} for 5 h) were measured using differential scanning calorimetry and found to be −8 °C for both the tri- and tetrafunctional thiol systems, well below the temperatures of interest (25−50 °C). In addition, the cured samples for both systems exhibited no crystallinity, thereby allowing us to interpret the rheological data in terms of gelation without interference from vitrification or crystallization.

Rheological Experiments. Rheological experiments were conducted using a Rheometrics Mechanical Spectrometer (RMS-800), fitted with a specially designed parallel plate fixture (Figure 3) in order to allow *in situ* monitoring of the photocrosslinking process. Both the top and bottom fixtures contained a quartz glass plate, 20 mm in diameter, which is transparent to the incident UV radiation. Removable screws held the quartz plates onto the fixtures. A section of the top fixture was cut away, allowing the incident radiation to be

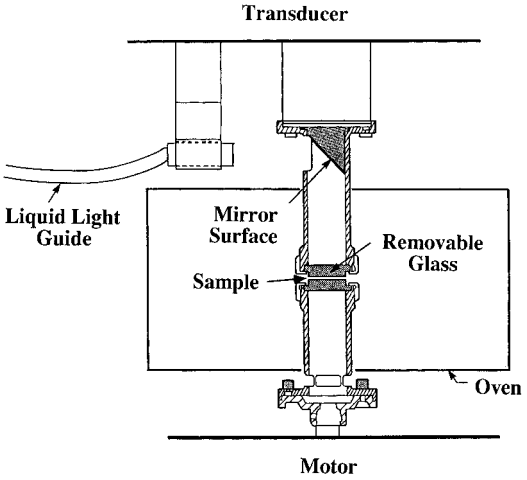

Figure 3. Schematic diagram of the specially designed parallel plate fixtures[10] utilized for *in situ* monitoring of UV cross-linking reactions. The incident UV radiation is reflected from the mirror onto the sample, which is placed between the two quartz plates.

directed onto the sample from a liquid light guide, via a mirror inclined 45° to the upper plate. The fixture was designed to be enclosed in the instrument oven, enabling experiments to be conducted at a controlled temperature. Photoinitiated polymerizations were conducted isothermally, at selected temperatures between 25 and 50 °C for the trifunctional thiol system and between 25 and 40 °C for the tetrafunctional thiol system. The sample thickness was held constant at 0.3 mm in all experiments.

A 200 W Oriel mercury lamp was used as the UV radiation source. A narrow band interference filter controlled the wavelength of the incident UV radiation. Neutral density filters were also used to attenuate the light intensity, which was measured using an International Light 1400A radiometer prior to commencing each experiment. Radial variation in the incident light intensity was observed to be less than ~7% in all cases. For all experiments, the intensity and wavelength of light was maintained at 0.15 mW cm^{-2} and 365 nm, respectively.

Fourier transform mechanical spectroscopy (FTMS)[11,12] was used to measure the evolving elastic, $G'(\omega,t)$, and viscous modulus, $G''(\omega,t)$, during photoinitiated polymerization. In this technique, an oscillatory strain, γ, is applied to the sample, such that

$$\gamma = \sum_{i=1}^{m} \gamma_i \sin(\omega_i t) \qquad \omega_1 = \omega_f, \quad \omega_2 = n_2\omega_f, \quad \ldots \quad \omega_8 = n_8\omega_f \tag{6}$$

The resulting stress is measured, and a discrete Fourier transform is performed to obtain the dynamic moduli. The experimental variables in FTMS are the fundamental frequency, ω_f, and the strain amplitudes, γ_i, at each frequency, ω_i. Each of the other frequencies are harmonics (integer multiples) of the fundamental frequency. The fundamental frequency was set at 1 rad/s, while the harmonics were chosen to be 3, 5, 10, 30, 70, and 100 rad/s. The corresponding strain amplitudes for each frequency were maintained at 5%, 5%, 5%, 3%, 2%, 2%, and 2%, respectively. The sum of the strain amplitudes was kept below a critical amplitude, γ_c, corresponding to the linear viscoelastic limit of the material, such that

$$\sum_{i=1}^{m} \gamma_i \le \gamma_c \tag{7}$$

The total strain of 24% in these experiments was well below the linear viscoelastic limits of both thiol−ene systems.

Results and Discussion

Effects of Temperature. Initial efforts focused on understanding the effects of temperature on the photoinitiated polymerization kinetics of the model thiol−ene systems. Only three previous studies[8,13,14] have considered how temperature affected the properties of the cross-linking polymer at its gel point. However, none of these studies addressed the effects of temperature on the real time kinetics of UV cross-linking systems. FTMS was initially used to monitor the UV cross-linking of trimethylolpropane tris(2-mercaptoacetate) in the presence of triallyl isocyanurate. The evolution of the elastic, $G'(\omega,t)$, and viscous modulus, $G''(\omega,t)$, over the course of the cross-linking reaction is shown in Figure 4. Following irradiation of the sample for 980 s, the viscous modulus is an order of magnitude larger than the elastic modulus over the entire frequency range, indicating that the material is in a pregel or sol state. At $t = 1480$ s, G' and G'' are parallel and show a power-law variation with respect to the frequency of oscillation (G', $G'' \sim \omega^n$), indicating the system to be at its gel point. The viscous modulus is greater than the elastic modulus at the gel point because $\tan(n\pi/2)$ (defined as G''/G') is greater than unity for $n > 0.5$ and less than unity for $n < 0.5$. For this system, n was determined to be 0.80. As the cross-linking progresses, G' eventually becomes larger than G'' ($t =$ 5155 s) and frequency independent, both of which are characteristics of a cross-linked system. The elastic modulus increases by more than three orders of magnitude during UV cross-linking, as the thiol−ene system is transformed from a viscous liquid to a highly cross-linked network.

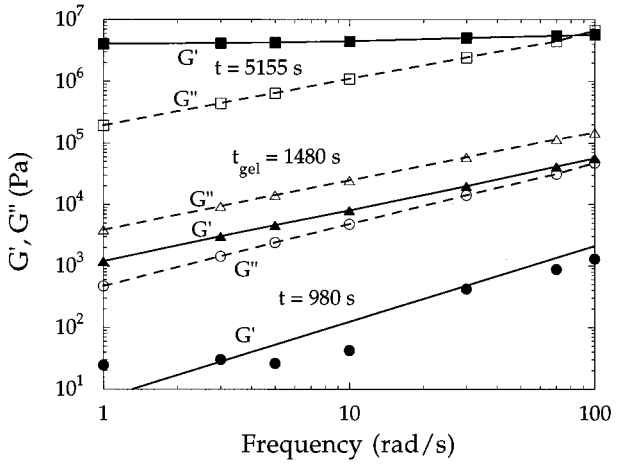

Figure 4. Elastic (G') and viscous (G'') moduli as a function of frequency plotted at three different UV exposure times for the trifunctional thiol system. At $t = 980$ s, G'' is larger than G' and the moduli are not parallel, corresponding to a material in the pregel state. G' and G'' are parallel at 1480 s, indicating that the sample is at the gel point. G' is independent of frequency and larger than G'' at 5155 s, indicating the sample is highly cross-linked. Here, $T = 35$ °C. Solid symbols correspond to G' and open symbols to G''.

The kinetics of the sol−gel transformation are more clearly represented when the elastic and viscous moduli are plotted as a function of exposure time at a constant frequency. This is illustrated in Figure 5. Here G'' is larger than G' at the onset of photoinitiated polymerization and the cross-linking rate is high. As the polymerization progresses, G' becomes larger than G'' and the rate of cross-linking slows appreciably. Two factors contribute to the decrease in the cross-linking rate. Firstly, as cross-linking progresses, the amount of reactive functionalities decreases, resulting in the decreased rate. Secondly, at higher conversions, the free radicals become incorporated into the cross-linking

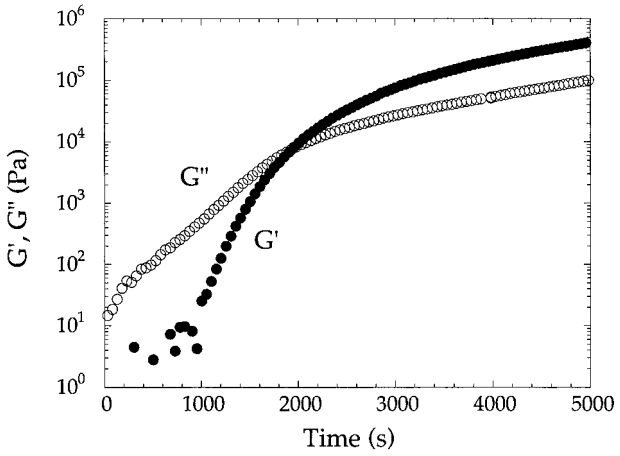

Figure 5. Evolution of the elastic (G') and viscous (G'') moduli as a function of exposure time for the trifunctional thiol system. The experimental temperature is 35 °C, and the frequency of oscillation is 10 rad/s. G'' is initially larger than G', but as the photo-cross-linking progresses, G' supercedes G''.

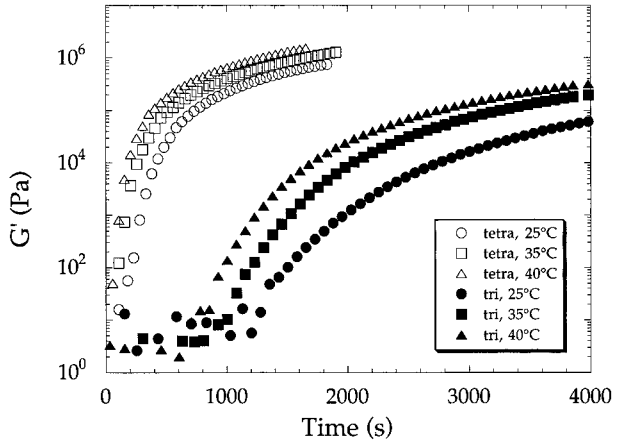

Figure 6. Comparison of the elastic modulus of the tri- and tetrafunctional thiol systems at different temperatures. The tetrafunctional thiol system cross-links much faster than the trifunctional thiol system for the temperatures studied. For both systems, increasing the temperature increases the cross-linking rate. Here, the frequency of oscillation is 10 rad/s.

network, thus reducing the mobility of the radicals. Since polymerization occurs when the radicals encounter a monomeric species, the reduced mobility of the radicals decreases the polymerization rate.

Figure 6 shows the effects of temperature on UV cross-linking for the tri- and tetrafunctional thiol systems. Here, the evolving elastic modulus is shown for three temperatures, 25, 35, and 40 °C. For the trifunctional thiol system, there is an initial induction period during which no changes in G' are observed. This induction period results from the hydroquinone which was added to the system to prevent premature polymerization. Hydroquinone inhibits cross-linking by reacting with free radicals to produce stable species, which no longer participate in the polymerization process. Once the hydroquinone in the system is depleted, cross-linking proceeds rapidly with an attendant rise in G'. Note that no appreciable induction times are seen for the tetrafunctional thiol system and photocross-linking proceeds at a faster rate, as evidenced by the more rapid growth in G'. Notably, the elastic moduli for the tetrafunctional thiol formulation attained a value of $\sim 10^5$ Pa before any detectable elastic component was observed for the trifunctional thiol system. Increasing

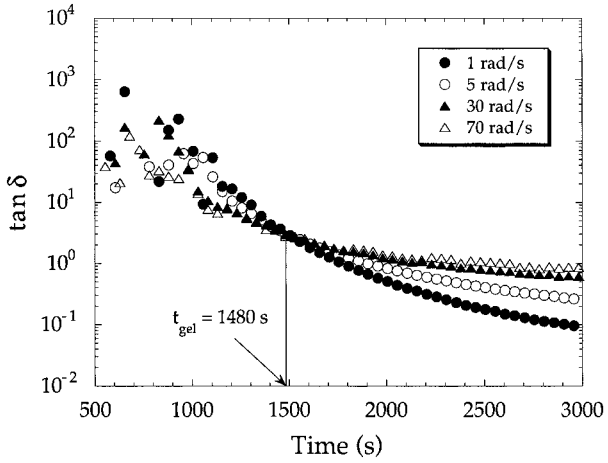

Figure 7. Loss tangent, tan δ, of the trifunctional thiol system plotted as a function of UV exposure time for different frequencies (as labeled in the figure). The intersection of tan δ at a single point ($t = 1480$ s) determines the gel point. Here, $T = 35$ °C.

Table 1. Gel Times for Different Reaction Temperatures

	gel time (s)	
temp (°C)	trifunctional thiol	tetrafunctional thiol
25	2160	310
30	1680	170
35	1480	150
40	1160	90
45	1030	
50	910	

the temperature increases the rate of cross-linking for both systems, as evidenced by the greater rate of increase of G' at higher temperatures. The time needed to reach a certain value of the moduli also decreases with increasing temperature.

Gel Point. It has been shown[7] that G' and G'' follow a power-law behavior with a common exponent, n, at the gel point. However, it is often difficult to precisely determine this point during the course of the experiment. The gel point can be determined by an alternative approach by taking advantage of the frequency independence of the loss tangent, tan δ, in eq 5. Figure 7 shows such a plot of tan δ, measured at several frequencies of oscillation, as a function of time for the trifunctional thiol system. The values of tan δ intersect at a time $t = 1480$ s, corresponding to the gel time, t_{gel}. The gel times for both the tri- and tetrafunctional thiol systems, at different temperatures, were obtained from tan δ plots similar to Figure 7 and are listed in Table 1. Increasing the temperature increases the rate of cross-linking. Consequently, at higher temperatures, the systems reach their gel points more quickly and the gel times are shorter. Also, the gel times for the tetrafunctional thiol system are shorter than for the trifunctional thiol system due to their faster cross-linking rates.

The relaxation exponents, n, at the gel point were also determined from tan δ plots and by using eq 5. For the trifunctional thiol system, the values of n remain constant at 0.80 throughout the temperature range studied. For the tetrafunctional thiol system, the values of n varied slightly from 0.81 to 0.82. This indicates that the properties of the critical gels for both systems do not depend on the temperature at which the cross-linking reaction is conducted. This suggests that within the experimental temperature ranges, the reaction mechanism in each case remains unchanged and the

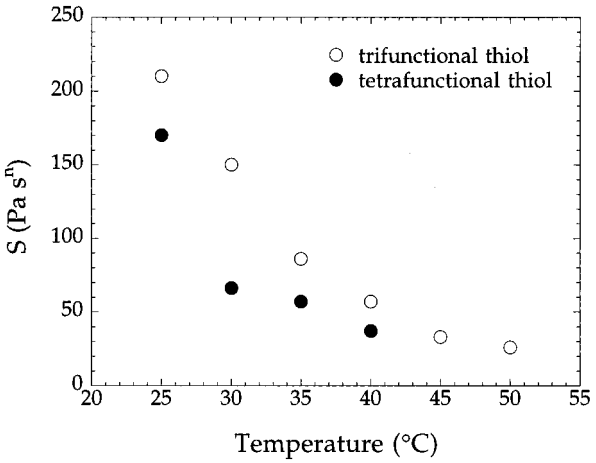

Figure 8. Gel stiffnesses, S, for the tri- and tetrafunctional thiol systems decrease with increasing temperature. The polymer strengths at the gel point for the tetrafunctional thiol system are always weaker (lower S) because of the lower conversion achieved.

extents of reaction at the gel point are constant.[13] The only effect of increasing temperature is to increase the rate of cross-linking. This independence of n with temperature may be used to simplify the study of temperature effects on the gelation of thiol−ene systems. The relaxation exponent, n, may initially be determined by performing one FTMS experiment at a suitable temperature where the cross-linking rate is not high. For other temperatures, the gel point may be subsequently determined by performing a dynamic time sweep at a fixed frequency and recording the point at which the ratio G''/G' ($\equiv\tan\delta$) passes through the previously determined value of $\tan(n\pi/2)$.

Another material parameter which characterizes the system at its gel point is the gel stiffness, S. The values of S for both systems studied were determined from eq 1 or 2 and are plotted as a function of temperature in Figure 8. The gel stiffness decreases with increasing temperature for both systems. This observation may be rationalized in terms of the empirically determined form of S,[15] given by

$$S = G_0\lambda_0^{\,n} \tag{8}$$

where G_0 is a material characteristic modulus. For end-linking systems, G_0 has a value close to the modulus of the fully cross-linked material (G_e). Scanlan *et al.*[15] also showed that $G_0\lambda_0$ is equal to the zero-shear viscosity of the prepolymer (η_0). If the reaction mechanism does not change throughout the temperature range studied, G_e remains constant with increasing temperature.[13] Since $\eta_0(T)$ decreases with increasing temperature, so should $S(T)$, as was observed for our systems.

The S values for the trifunctional thiol system are greater than those for the tetrafunctional thiol system over the temperature range studied. This can be explained in terms of the Flory−Stockmayer theory of gelation. This theory predicts the degree of conversion at the gel point for the thiol−ene systems, by means of the following expression:[16]

$$x_c = \frac{1}{[r(f_{\text{thiol}} - 1)(f_{\text{allyl}} - 1)]^{1/2}} \tag{9}$$

where x_c is the critical extent of conversion at the gel point, r is the stoichiometric ratio of thiol groups to allyl groups, f_{thiol} is the functionality of the thiol monomer, and f_{allyl} is the functionality of the allyl monomer. For a stoichiometric ratio of 1, eq 9 predicts values of x_c equal to 0.50 for a trifunctional thiol/trifunctional allyl system and x_c equal to 0.41 for a tetrafunctional thiol/trifunctional allyl system. Since a higher conversion is achieved for the trifunctional thiol system at its gel point, it should possess a higher cross-link density and, therefore, a greater gel stiffness than that of the tetrafunctional thiol system (Figure 8).

The power-law variation of the dynamic moduli at the gel point has led to theories suggesting that the cross-linking clusters at the gel point are self-similar or fractal in nature.[17] Percolation models have predicted that, at the percolation threshold, where a cluster expands through the whole sample (i.e. gel point), this infinite cluster is self-similar.[17] The cluster is characterized by a fractal dimension, d_f, which relates the molecular weight M of the polymer to its spatial size R, such that

$$R^{d_f} \sim M \tag{10}$$

The fractal dimension measures how open or packed a structure is; lower fractal dimensions indicate a more open system, while higher fractal dimensions indicate a more packed system.[17] Theories relating the fractal dimension to the relaxation exponent, n, have been put forward. These are based on whether the excluded volume of the polymer chains is screened or unscreened under conditions near the gel point.[18] It is known that the excluded volume of a polymer chain is progressively screened as its concentration is increased, the size of the chain eventually approaching its unperturbed dimensions. Such screening is expected to occur near the gel point, since cross-linked clusters of varying sizes are present and the situation is similar to that encountered in a polymer melt, as far as the excluded volume effects are concerned.[18] For the case when the excluded volume is fully screened, the relaxation exponent, n, can be related to the fractal dimension, d_f, at the gel point by[18]

$$n = \frac{d(d + 2 - 2d_f)}{2(d + 2 - d_f)} \tag{11}$$

where d is the space dimension, which in this case is 3. By applying eq 11, fractal dimensions of 1.6 are obtained for both the tri- and tetrafunctional thiol systems. The same fractal dimension suggests that the cross-linked structures produced at the gel point are similar for both systems. This is somewhat surprising since one would expect the tetrafunctional thiol network structure to be more branched, and consequently have a lower fractal dimension, due to its lower conversion at the gel point. Although the tetrafunctional thiol system has a lower conversion and, consequently, a lower S at the gel point, it seems that the infinite clusters of both systems exhibit similar packing.

Activation Energy. Since the relaxation exponents remain independent of temperature for both formulations, one can conclude that the extent of reaction at the gel point is also temperature independent.[13] From the gel times calculated at different temperatures, we can then determine apparent activation energies for the two systems. The polymerization reaction can be represented by a generalized kinetic expression of the type:[19]

$$\frac{dx}{dt} = k\, f(x) \qquad k = A \exp(-E/RT) \qquad (12)$$

where x is the extent of reaction, k is the rate constant, t is the time of reaction, $f(x)$ represents an arbitrary functional form for the extent of reaction, T corresponds to the temperature of the reaction, A is the preexponential factor, and E is the apparent activation energy. Equation 12 can be integrated from the onset of the cross-linking reaction (time $t = 0$, $x = 0$) to the gel point ($t = t_{gel}$, $x = x_c$) to obtain

$$\ln t_{gel} = \ln\left(\int_0^{x_c} dx/f(x)\right) - \ln(A) + E/RT \qquad (13)$$

Thus, a semilogarithmic plot of the gel time as a function of $1/T$ should exhibit a linear relationship with the slope corresponding to the apparent activation energy. Such a plot is illustrated in Figure 9 for both the tri- and tetrafunctional thiol systems. An apparent activation energy of 6.6 kcal/mol is obtained for the trifunctional thiol system, which is less than the value of 13.9 kcal/mol determined by Hoyle *et al.*[4] for a different thiol monomer, trimethylolpropane tris(3-mercaptopropionate). They also used a different technique, differential scanning calorimetry, to determine the apparent activation energy. For the tetrafunctional thiol system, an apparent activation energy of 14 kcal/mol is obtained, more than twice the value for the trifunctional thiol system.

Although the tetrafunctional thiol system exhibits a larger apparent activation energy, it still cross-links at a faster rate than the trifunctional thiol system, as evidenced from the time dependent elastic modulus shown in Figure 6. A possible explanation for this behavior may lie in the transition state theory,[20] where the rate constant, k, for a reaction is given by

$$k = \frac{\kappa T}{h} e^{-\Delta G^{\ddagger}/RT} \qquad (14)$$

where κ is the Boltzmann constant, T is the reaction temperature, h is the Planck constant, $\Delta G^{\ddagger}$ is the free energy of activation, and R is the gas constant. Thus, it is the free energy of activation and not necessarily the heat of activation which determines the reaction rate at a given temperature. The free energy of activation can be expressed in terms of an entropy ($\Delta S^{\ddagger}$) and an enthalpy ($\Delta H^{\ddagger}$) of activation, and the enthalpy of activation can in turn be expressed in terms of the experimental activation energy, E,[20] such that

$$k = e\frac{\kappa T}{h} e^{\Delta S^{\ddagger}/R} e^{-E/RT} \qquad (15)$$

Therefore, a balance between the entropy of activation, $\Delta S^{\ddagger}$, and the apparent activation energy, E, dictates the magnitude of the rate constant. This has been observed for other systems.[21,22] The entropy of activation is a measure of the difference in the entropies of the activated complex and the reactants. A positive value of $\Delta S^{\ddagger}$ implies that the entropy of the activated complex is greater than that of the reactants. More often, the entropy decreases with the formation of an activated complex. Due to the faster cross-linking rate of the tetrafunctional thiol system, it may be inferred that $\Delta S^{\ddagger}$ is necessarily larger for this system. This offsets the higher activation energy determined for the tetrafunctional thiol system, consistent with the higher observed cross-linking rates.

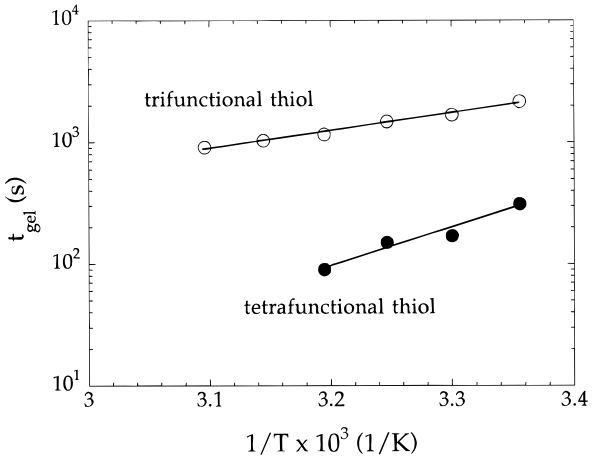

Figure 9. Semilogarithmic plot of the gel times (t_{gel}) as a function of $1/T$ to determine the apparent activation energies of UV cross-linking for the two systems. Activation energies are found to be 6.6 and 14 kcal/mol for the tri- and tetrafunctional thiol systems, respectively.

Conclusions

We have utlized a novel, *in situ* technique to probe the evolving rheological properties of UV cross-linking thiol−ene polymers and related macroscopic properties of the polymer to other quantities, such as fractal dimensions, activation energies, and gel times. Utilizing Fourier transform mechanical spectroscopy, we monitored the UV cross-linking of two thiol−ene systems, one containing a trifunctional thiol and the other containing a tetrafunctional thiol. We find the tetrafunctional thiol system to exhibit a faster cross-linking rate than the trifunctional thiol system. We also examined the effects of temperature on these reactions and the cross-linking rates are found to increase with increasing temperature.

We determined the gel times, t_{gel}, the gel stiffnesses, S, and the relaxation exponents, n, by applying the Winter−Chambon criterion at the gel point. The gel stiffness for the trifunctional thiol system is greater than those for the tetrafunctional thiol system over the range of temperatures studied because of the higher conversions achieved at the gel point. Relaxation exponents of 0.80 and 0.81−0.82 were determined for the tri- and tetrafunctional thiol systems, respectively. The exponents are found to be independent of the temperature for both systems, suggesting that the reaction mechanisms remained unchanged over the temperature range studied. The fractal dimensions, calculated from the relaxation exponents, are the same for both systems, indicating similar packing of the network at the gel point.

From the gel times, we calculated apparent activation energies of 6.6 kcal/mol for the trifunctional thiol system and 14 kcal/mol for the tetrafunctional thiol system. We hypothesize that a greater entropy of activation for the tetrafunctional thiol system compensated for its larger apparent activation energy, consistent with the faster cross-linking rate observed for the tetrafunctional thiol system.

Acknowledgment. We thank the American Chemical Society Petroleum Research Fund and a GAANN Fellowship for financial support of this work.

References and Notes

(1) Jacobine, A. F. In *Radiation Curing in Polymer Science and Technology*; Fouassier, J. B., Rabek, J. F., Eds.; Elsevier Science Publishers Ltd.: New York, 1993; Vol. III, p 219.
(2) Morgan, C. R.; Magnotta, F.; Ketley, A. D. *J. Polym. Sci., Polym. Chem. Ed.* **1977**, *15*, 627.
(3) Hoyle, C. E.; Hensel, R. D.; Grubb, M. B. *Polym. Photochem.* **1984**, *4*, 69.
(4) Hoyle, C. E.; Hensel, R. D.; Grubb, M. B. *J. Polym. Sci., Polym. Chem. Ed.* **1984**, *22*, 1865.
(5) Jacobine, A. F.; Glaser, D. M.; Grabek, P. J.; Mancini, D.; Masterson, M.; Nakos, S. T.; Rakas, M. A.; Woods, J. G. *J. Appl. Polym. Sci.* **1992**, *45*, 471.
(6) Rakas, M. A.; Jacobine, A. F. *J. Adhesion* **1992**, *36*, 247.
(7) Winter, H. H. Gel Point. In *Encyclopedia of Polymer Science and Engineering*; John Wiley & Sons: New York, 1989.
(8) Winter, H. H.; Chambon, F. *J. Rheol.* **1986**, *30*, 367.
(9) De Rosa, M. E.; Winter, H. H. *Rheol. Acta* **1994**, *33*, 220.
(10) Khan, S. A.; Plitz, I. M.; Frantz, R. A. *Rheol. Acta* **1992**, *31*, 151.
(11) Holly, E. E.; Ventkataraman, S. K.; Chambon, F.; Winter, H. H. *J. Non-Newtonian Fluid Mech.* **1988**, *27*, 17.
(12) In, M.; Prud'homme, R. K. *Rheol. Acta* **1993**, *32*, 556.
(13) Izuka, A. I.; Winter, H. H.; Hashimoto, T. *Macromolecules* **1994**, *27*, 6883.
(14) Ragahavan, S. R.; Chen, L. A.; McDowell, C.; Khan, S. A.; Hwang, R.; White, S. Rheological Study of Cross-Linking and Gelation in Chlorobutyl Elastomer Systems. *Polymer*, in press.
(15) Scanlan, J. C.; Winter, H. H. *Macromolecules* **1991**, *24*, 47.
(16) Odian, G. *Principles of Polymerization*; John Wiley & Sons: New York, 1981.
(17) Feder, J. *Fractals*; Plenum Press: New York, 1988.
(18) Muthukumar, M. *Macromolecules* **1989**, *22*, 4656.
(19) Oyanguren, P. A.; Williams, R. J. J. *J. Appl. Polym. Sci.* **1993**, *47*, 1361.
(20) Glasstone, S.; Laidler, K. J.; Eyring, H. *The Theory of Rate Processes*; McGraw-Hill Book Co.: New York, 1941.
(21) Annable, T.; Buscall, R.; Ettalaie, R.; Whittlestone, D. *J. Rheol.* **1993**, *37*, 695.
(22) Hunter, R. J. *Foundations of Colloid Science*; Clarendon: Oxford, U.K., 1987.

MA960383E